ISSN 1067-8212, Russian Journal of Non-Ferrous Metals, 2015, Vol. 56, No. 3, pp. 261–266. © Allerton Press, Inc., 2015.

METALLURGY OF NONFERROUS METALS

The Effect of Different Melt Treatments on Alloying Element Distribution and Mechanical Properties of A356 Aluminum Alloy[1]

M. Khodaei[a, *] **and N. Parvin**[b, **]

[a] *Department of Materials Science and Engineering, Islamic Azad University, Majlesi branch, Isfahan, Iran*
[b] *Mining and Metallurgical Engineering Department, Amirkabir University of Tech., Tehran, Iran*
*e-mail: *M.Khodaei@ma.iut.ac.ir, **nparvin@aut.ac.ir*

Received November 6, 2014

Abstract—It is widely believed that needle plates of Fe-rich intermetallic compounds decrease the mechanical properties in A356 aluminium alloys. Moreover, the cooling rate has significant effect on the microstructure and the mechanical properties of this alloy and it can make the Fe-rich intermetallic compounds finer. In this research the synergic effect of cooling rate and ultrasonic power and mechanical vibration on the microstructure of A356 has been investigated. Ultrasonic power was applied to the melt by a novel bath type ultrasonic power system. The distribution of alloying elements has also been studied by scanning electron microscope (SEM) and it has been analyzed by EDS. Mechanical properties of samples were investigated by hardness and tensile tests. Results indicate that ultrasonic power effectively modified the microstructure of A356 and it has better efficiency than mechanical vibration. The Fe-rich phases in ultrasonically treated samples had the finest morphologies in the range of 10 micrometer. Ultrasonic power improves mechanical properties of samples even more than mechanical vibration. Comparison the obtained results with the results of other researchers, it is concluded that bath type ultrasonic power system are more effective than probe type ones.

Keywords: alloying element distribution, A356 aluminum alloy, ultrasonic treatment, mechanical vibration

DOI: 10.3103/S1067821215030098

1. INTRODUCTION

A356 aluminum alloy is one of the widely used casting aluminum alloys because of its good mechanical properties such as ductility, hardness, fatigue strength, pressure tightness, melt fluidity, and machinability [1].

The microstructure gives useful information on the quality of the cast. After every melt treatment the microstructure can be investigated to assess the treatment effect. Fine and equiaxed grains are believed to be more appropriate in castings. The size and shape of eutectic Silicon phase has a major role in the variation in the mechanical properties of A356 alloy [2]. Fine structures raise strength and ductility [3]. Grain refining is a common practice to ameliorate the mechanical properties of casting parts. Fine equiaxed grains in the castings improve feeding ability, uniformed distribution of second phases and micro porosity, and uniformity of properties and machinability [4].

As mentioned above, some researchers investigated the size of dendritic silicon phase and the others investigated the size of primary α phase in A356 aluminum alloy treated by different methods.

The first reported case of sinusoidal vibration of steel molds was by Chernov (1968) who refined the primary austenite. Other researchers report that by implementation of mechanical vibration, the nucleation rate increased and grain size and porosity size decreased. Mechanical vibration leads to the average grain size of the primary phase became finer and more globular as the degree of vibration increased [5].

According to the results of Dheir et al. [6], with increasing mechanical vibration amplitude, Silicon morphology will be closer to fibrous forms in A356. Of course if vibration amplitude reached a certain limit, Silicon phases will be coarser. Controlling and optimization of the microstructure in the casting as well as considering economic parameters will lead to increase in the quality of final products.

Taghavi et al. [7] reported that by increasing vibration frequency from 10 to 50 Hz and the time of vibration to 15 minutes, the size of primary α phase of A356 alloy can be reduced to 173 μm. They suggested that the best condition can be achieved in 50 Hz and 15 minutes of mechanical vibration.

Jian et al. [8] held molten A356 alloy in the pasty region (isotherm condition between solidus and liquidus) under ultrasonic vibration and reduced the aver-

[1] The article is published in the original.

age grain size but failed to produce a globular microstructure, A globular/non-dendritic microstructure was obtained and grains were refined in the melt subjected to a continuous acoustic vibration when the melt was cooled from liquidus to solidus.

Jian et al. [9] also used ultrasonic power to modify the microstructure of A356 alloy which poured in permanent copper mold and reduced the size of eutectic silicon phase from 26 μm to 2 μm in length.

Zhang et al. [10] indicated that the long dendritic silicon phases of A356 can be broken into pieces and a considerable improvement in mechanical properties can be achieved due to the ultrasonic treatments. They used ultrasonic power system from the upper side of the molten metal in the furnace. The fracture mechanisms of the as-prepared A356 alloys were changed from cleavage fracture to dimple fracture, especially, when the value of the ultrasonic power was 1.2 kW.

Zhang et al. [11] showed that by generating an endothermic transformation in the cooling media, more favorable results can be achieved as compared to that of, water cooling copper molds.

There are many techniques to refine grains in Aluminum alloys, which can be classified into three groups namely; thermal, chemical and dynamic methods.

Vibration activates oscillation in different points of molten metal and generates extensive nucleation sites. According to Clausius-Clapeyron's equation, localized pressure rise due to vibration can raise the melting point instantaneously. This phenomenon makes a great under cooling, and also breaks dendrite arms. The broken arms act as good nuclei themselves since their compositions are homogeneous and have a high wettability with the melt. Another paper by Fan [12], explained the grain refinement in melts under turbulence, who investigated conditions for severe turbulence in the melt. In other words, effective nucleation rate is greater in the melts under turbulence.

Ultrasonic power can generate transient acoustic cavitation in the melt and this phenomenon is responsible for refining microstructures, degassing of liquid metals, and dispersive effects for homogenizing. Yang et al. [13] use ultrasonic power to disperse nanoparticles in the molten metal. While ultrasonic is applying in the melt, the behaviors of the diffusion and mass transfer can be changed. Also the pressure fluctuates and heat disturbance effect of ultrasonic treatment, the growing dendrite arms are broken into fine particles. So the growth of dendrite can be restrained effectively and metallic melt solidifies and forms fine equiaxed microstructure [14].

Gao et al. [15] applied 0 W to 700 W ultrasonic power on AZ91 alloy in sand mold and reduce grain size from 202 to 146 micrometer. They obtained globular grains in AZ91 alloy subjected to the high density ultrasonic vibration (probe type ultrasonic power system), and this, increased UTS from 145 to 195 MPa.

Zhao-hui et al. [16] found that the best condition for ultrasonic application (probe type ultrasonic power system) is power of 600 W and 100 s in a type of Mg alloy. They introduced ultrasonic power from the top of the magnesium melt with a cylindrical probe made of the tool steel. They claimed that the cavitation and acoustic streaming caused by ultrasonic treatment play a major role in refining the microstructure and increasing mechanical properties of the alloy.

Lei et al. [17] found that the best condition for ultrasonic application is power of 170 W in 90 s in a type of Mg alloy during its solidification process. They poured melt in a steel mold and introduced ultrasonic power from the top of the magnesium melt with a cylindrical probe made of the stainless steel.

Puga et al. [3] used MMM[2] ultrasonic technology to refine the grains of an aluminium alloy. They investigated the effect of treatment temperature and electric power. They reduced the primary alpha grain size to 41 μm by using 600 W ultrasonic power at 615°C melt temperature. Their ultrasonic system was probe type and used it in constant temperatures.

All previous researches have used probe type ultrasonic power, but we have used a transducer was installed under the bath. A little water for transducer chilling (5 mm depth) and the steel mold placed in the bath. This system will apply ultrasonic waves to the melt directly.

Feng et al. [18] used a crucible that directly attached to the Ultrasonic Transducer to refine the morphology of hypereutectic Al—23%Si alloy. They observed that the hydrogen bubbles in the alloy melt were removed, the primary Si phase was refined and the eutectic lamellar spacing increased. It is thought that the vibration was transmitted to the melt mechanically by means of crucible walls, and there were no ultrasonic power in the melt.

Based on the past literature, it appears that more work on other aspects of the vibration of molten metals is needed to be carried out.

In this research the effect of bath type ultrasonic treatment, mechanical vibration and mold materials on the microstructure of A356 aluminium alloy has been investigated. For this objective a novel setup of a bath type sonicator was used during solidification process. Also X-ray map is used to clarify that except dendritic silicon phase and primary α phase, is there anything to change by ultrasonic power or not.

2. MATERIALS AND METHODS

In this study a gas fired furnace was used for melting A356 aluminium alloy to the nominal composition as illustrated in Table 1. The pouring temperature was set on 700°C into a 2 kg graphite crucible under the conditions given in Table 2.

[2] Multi-frequency, Multimode, Modulated.

Different mold conditions are summarized below:

Mold 1: A metallic stainless steel mold having 0.5 mm wall thickness was cooled in air.

Mold 2: A metallic stainless steel mold having 0.5 mm wall thickness was placed in an ultrasonic bath which was maintained to complete solidification of the melt (Fig. 1). Actually the used system was not probe type and the whole metallic mold was placed in the bath of sonicator.

Mold 3: A silica sand (AFS 90) mold with sodium silicate binder.

Mold 4: A metallic stainless steel mold having 0.5 mm wall thickness was vibrated mechanically in air (amplitude: 0.6 mm and frequency 50 Hz).

After casting and solidification, samples (with 6 cm height and 3 cm diameter) were extracted from the molds and cut.

Samples were polished and etched by 10% HF etchant solution and were studied by scanning electron and optical microscopes.

The morphology of phases and microstructural characteristics of all samples were examined by Scanning Electron Microscope (SEM) (SERON TECH. AIS 2100) using secondary electron detector. X-Ray map was performed using EDX (equipped to the SEM) to distinguish the alloying element distribution.

The hardness of the samples was measured by Brinel hardness test (indenter diameter 2.5 mm and final applied load 100 kgf). Hardness test was carried out 3 times for each sample and the average was reported.

Tensile test on cylindrical samples (6 mm diameter and 9 mm height) were performed using a Universal Testing Machine (HOUNSFIELD: H30KS) according to ASTM E8 at a crosshead speed of 1 mm min^{-1}. Ultimate tensile strength and yield strength were determined based on engineering stress-strain curves. This test was carried out three times to obtain the average values.

Table 1. A356 nominal chemical analysis

Element	Al %	Si %	Mg %	Cu %	Fe %	Mn %	Ti %
Wt %	Rem.	6.5–7.5	0.25–0.45	<0.2	<0.2	<0.1	<0.2

Table 2. Different molding conditions

Mold number	Mold materials	Treatment or cooling media
Mold 1	Steel	Air
Mold 2	Steel	Ultrasonic power
Mold 3	Silica sand	Sand
Mold 4	Steel	Mechanical vibration

3. RESULTS AND DISCUSSION

The optical micrographs of samples are shown in Fig. 2. The finest dendrite arm appeared in sample 2. Optical micrographs revealed the Silicon and Fe-rich intermetallic compounds. However, this was not clearly distinguishable that which one is Fe-rich or silicon. Thus the Fe-rich intermetallic phases in all samples investigated by EDS X-Ray map (Fig. 3).

The hardness values of the samples, solidified under ultrasonic power were generally high as compared with the other conditions.

Nevertheless mold 1 has metallic walls, and high heat transfer rate was expected, but apparently in mold 1 two factors reduced the rate of heat transfer during solidification. The mold wall was so thin that the mold temperature reached the melt temperature rapidly, and the second factor was related to air gap generation between mold wall and sample during solidification (because of metal contraction during solidification).

The second highest hardness was associated with mechanically vibrated mold. Observations indicated that mechanical vibration was not as effective as ultrasonic power. However, it made a better condition than static molds. Mechanical vibration also can collapse dendrite arms during solidification and disperse them in the melt.

Dispersed broken dendrite arms act as nuclei's in the melt and produce finer grains and microstructure. Vibration led to the breakage of dendrite arms and dispersed them in the melt.

The hardness test accuracy was ±2 HB and the hardness for molds 1 to 4 were 55, 104, 57, 80 HB, respectively (Table 4).

Results of metallographic studies and hardness tests show that net shaped silicon phase in ultrasonically treated sample was the major reason for highest hardness. On the other hand fine silicon phases as

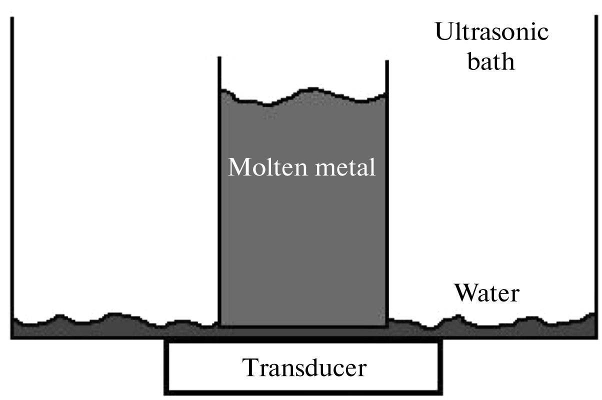

Fig. 1. Mold and ultrasonic power system.

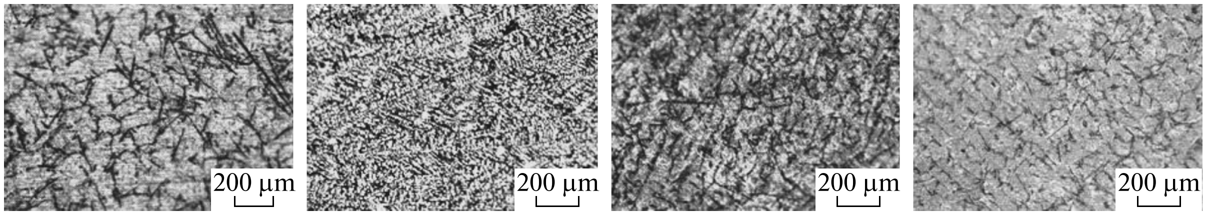

Fig. 2. A356 aluminium alloy microstructures in different treatment conditions (sample 1 in the left and sample 4 in the right).

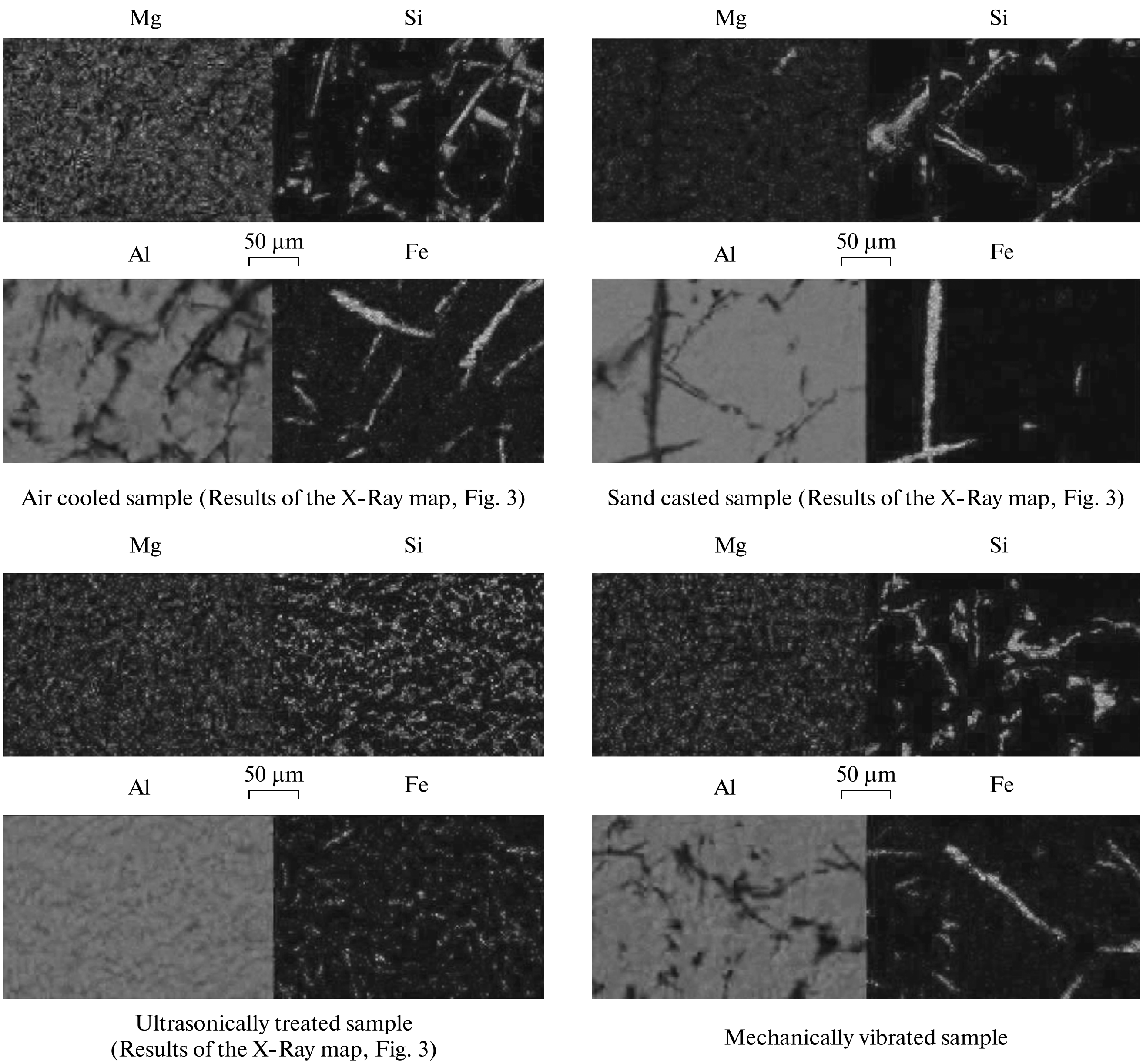

Fig. 3. Results of the X-Ray map.

shown in map images dispersed in the matrix. This particles act as barriers for dislocations motion (Fig. 3). These barriers restrict the motion of dislocations and increase the hardness of metal. The homogeneity of mechanically vibrated mold in sample 4 was greater than molds 1 and 3 but it was not as fine as sample 2.

Alloying element distributions are shown in Fig. 3 which illustrates that ultrasonic vibration has had a great influence on the distributions of alloying elements such as Iron.

Based on the optical micrographs, the phase type is not distinguishable. X-ray mapping revealed Magnesium in red, Silicon in green, aluminium in blue and Iron in magenta color.

As seen in Fig. 3, sample 2 has the most homogenous distributions of alloying elements, especially Iron. In this sample, homogenous distributions of Fe-rich intermetallic compounds inhibit the formation of coarse Fe-rich intermetallic compounds such as β.

According to Fig. 3, magnesium was dispersed homogenously in all samples. In contrast, the distributions of Iron and silicon were not homogenous and they did not solve in the matrix. Fe and Si rich regions had less aluminium.

Figure 4 and Table 3 show the results of spot analysis by EDS. It can be found that the analyzed phases were not completely on the surface of specimen or their depth were smaller than 3 μm (the depth of electron beam diffusion in sample). Results of X-Ray maps clearly confirm the existence of silicon; However EDS analyses suggest the existence of other elements such as aluminum. This phenomenon may stem from the following origins:

Table 3. Results of spot analysis by EDS

Wt % in point 2	Wt % in point 1	Element
19.01	54.90	Al
80.55	15.55	Si
0.065	29.13	Fe
0.36	0.41	Mg
100.00	100.00	Total

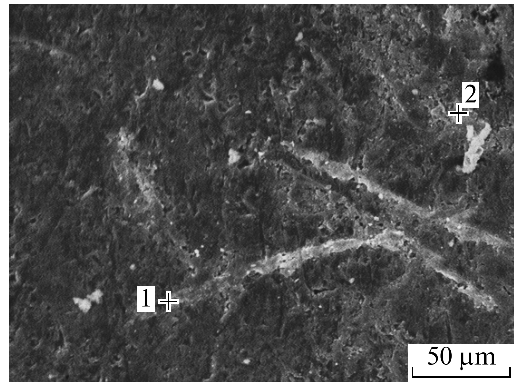

Fig. 4. The position of EDS spot analysis in sample 1.

(1) A thin layer of aluminium coating on silicon particles.

(2) The thickness of silicon is too low that the electron beam could pass through it detecting aluminium matrix.

According to results of spot analyze No. 1 in sample 1, there was some Silicon in Fe-rich phases. Of course in X-Ray maps, Fe and Si have no overlaps.

Results of sample 2 in Fig. 3 indicate that ultrasonic power break dendrite arms and some phases. Thus finer Si phases and Fe-rich intermetallic compounds formed in the matrix.

Fe-rich intermetallic compounds in other samples (except sample 2) are coarser than sample 2. And even mechanical vibration could not break Si phases completely. The micrographs of sample 4 in Figs. 2 and 3 indicate that mechanical vibration reduced the size of primary a phase and improve the mechanical properties. In Fig. 3, the left down image of each sample is related to SEM photographs (with SE detector) in ×500.

According to these Figures the size of α phase (that there is between dendrite arms) for samples 1 to 4 are 200, 15, 130 and 110 μm respectively. The size of primary α phase can reach to one tenth by ultrasonic power. Ultrasonic power during solidification can reduces the primary α and secondary phase's size effectively.

Mechanical properties of each condition are presented in Table 4. Ultimate tensile strength and yield

Table 4. Mechanical properties of samples

Mold number	Casting condition	Tensile strength-UTS (MPa)	Yield strength (MPa)	Hardness (HB)
Mold 1	Air	185	95	45
Mold 2	Ultrasonic power	303	210	104
Mold 3	Sand	199	105	57
Mold 4	Mechanical vibration	245	170	80

strength are reported based on average value of three times testing. It is evident that ultrasonically treated samples have higher mechanical properties, and it is in good agreement with the results of hardness test.

The hardness of ultrasonically treated sample is 56% higher than air cooled sample. The hardness of silica sand casted sample is 21% higher than air cooled sample and mechanically vibrated sample hardness is 43% higher than air cooled sample.

Based on a work by Jian et al. [8] on Al-Si alloy, it was concluded that the bath type ultrasonic power has more advantages in producing finer grains and higher mechanical properties than as compared to that of probe type.

4. CONCLUSIONS

Melt of the A356 aluminum alloy was treated in different ways in the present study, and their mechanical properties were investigated. The following conclusions can be drawn:

The Fe-rich intermetallic compounds tend to precipitate in the form of large particles in customary sand casting. Ultrasonic power can produce the finest intermetallic phases in the matrix.

Bath type ultrasonic power is superior in breaking secondary phases as compared to mechanical vibration and even probe type sonicators.

Thin wall metallic molds cooled in the air, have not high enough heat transfer rate to reduce the grain size effectively.

By using ultrasonic power on solidifying A356 samples, except dendritic silicon phase and primary α phase, Fe-rich intermetallic phases will be fine.

5. ACKNOWLEDGMENTS

The authors gratefully acknowledge the SEM Lab. of Islamic Azad University-Majlesi Branch.

REFERENCES

1. Gruzleski, J.E., Closset, B.M., and Schaumburg, I.L., *American Foundrymen's Society*, 1990, vol. 17.
2. Chul Park, C., Kim, S., Kwon, Y., Lee, Y., and Lee, J., *Materials Science and Engineering A*, 2005, vol. 391, p. 86, DOI: 10.1016/j.msea.2004.08.056.
3. Puga, H., Costa, S., Barbosa, J., Ribeiro, S., and Prokic, M., *Journal of Materials Processing Technology*, 2001, vol. 211, p. 1729, DOI: 10.1016/j.jmatprotec.2011.05.012.
4. Wang, J., He, S., Sun, B., Guo, Q., and Nishio, M., *Journal of Materials Processing Technology*, 2003, vol. 141, p. 29, DOI: 10.1016/S0924-0136(02)01007-5.
5. Limmaneevichitr, C., Pongananpanya, S., and Kajornchaiyakul, J., *Materials and Design*, 2009, vol. 30, p. 3925, DOI: 10.1016/j.matdes.2009.01.036.
6. Abu Dheir, N., Khraisheh, M., Saito, K., and Male, A., *Material Science and Engineering A*, 2005, vol. 393, p. 109, DOI: 10.1016/j.msea.2004.09.038.
7. Taghavi, F., Saghafian, H., and Kharrazi, Y.H.K., *Materials & Design*, 2009, vol. 30, p. 1604, DOI: 10.1016/j.matdes.2008.07.032.
8. Jian, X., Xu, H., Meek, T.T., and Han, Q., *Materials Letters*, 2005, vol. 59, nos. 2–3, p. 190, DOI: 10.1016/j.matlet.2004.09.027.
9. Jian, X., Meek, T.T., and Han, Q., Scripta Materialia, 2006, vol. 54, p. 893, DOI: 10.1016/j.scriptamat.2005.11.004.
10. Zhang, S., Zha, Y., Cheng, X., Chen, G., and Dai, Q., *Journal of Alloys and Compounds*, 2009, vol. 470, p. 168, DOI: 10.1016/jjallcom.2008.02.091.
11. Zhang, L.Y., Zhou, B.D., Zhan, Z.J., Jia, Y.Z., Shan, S.F., Zhang, B.Q., and Wang, W.K., *Materials Science and Engineering A*, 2007, vol. 448, p. 361, DOI: 10.1016/j.msea.2006.10.025.
12. Fan, Z., *International Materials Review*, 2002, vol. 47, no. 2, p. 49, DOI: 10.1179/095066001225001076.
13. Yang, Y., Lan, J., and Li, X., *Materials Science and Engineering A*, 2004, vol. 380, p. 378, DOI: 10.1016/j.msea.2004.03.073.
14. Li, Y.L., Feng, H.K., Cao, F.R., Chen, Y.B., and Gong, L.Y., *Materials Science and Engineering A*, 2008, vol. 487, p. 518, DOI: 10.1016/j.msea.2007.11.067.
15. Gao, D., Li, Z., Han, Q., and Zhai, Q., *Materials Science and Engineering A*, 2009, vol. 502, p. 2, DOI: 10.1016/j.msea.2008.12.005.
16. Zhao-hui, W., Xu-dong, W., Qing-feng, W., and Wen-bo, D., *Trans. Nonferrous Met. Soc. China*, 2011, vol. 21, p. 773, DOI: 10.1016/S1003-6326(11)60779-6.
17. Lei, Y., Hai, H., Shou-hua, J., Can-feng, F., and Xing-guo, Z., *Trans. Nonferrous Met. Soc. China*, 2011, vol. 21, p. 1241, DOI: 10.1016/S1003-6326(11)60848-0.
18. Feng, H.K., Yu, S.R., Li, Y.L., and Gong, L.Y., *Journal of Materials Processing Technology*, 2008, vol. 208, p. 330, DOI: 10.1016/j.jmatprotec.2007.12.121.